EVALUATION OF LAMINATED VENEER LUMBER TENSILE STRENGTH USING OPTICAL SCANNING AND COMBINED OPTICAL-ULTRASONIC TECHNIQUES

David B. DeVallance†

Assistant Professor
Division of Forestry and Natural Resources
West Virginia University
Morgantown, WV 26506

James W. Funck†

Unit Manager, Nondestructive Evaluation
Weyerhaeuser NR Company
Federal Way, WA 98063
and
Courtesy Faculty
Department of Wood Science and Engineering
Oregon State University
Corvallis, OR 97331

James E. Reeb

Associate Professor
Forestry and Natural Resources
Oregon State University Lincoln County Extension
Newport, OR 97365

(Received September 2010)

Abstract. Nondestructive commercial ultrasonic grading provides laminated veneer lumber (LVL) manufacturers a means for sorting veneer based on average ultrasonic propagation time (UPT) and/or average dynamic modulus of elasticity (MOE_d). However, little is known about the influence of veneer defects on strength properties of veneer and LVL. Including veneer defect and growth ring pattern measurements, obtained via optical scanning, was hypothesized to improve LVL static tensile strength (F_t) property predictions. Nondestructive and destructive testing of Douglas-fir (*Pseudotsuga menziesii*) veneer and LVL was performed to evaluate improvements in LVL F_t property predictions. Various models based solely on density, optical, ultrasonic, and combined system measurements were developed for LVL property predictions. LVL static F_t was best predicted ($R^2 = 0.65$) with integrated optical and ultrasonic measurements (ie combined system model), which included average defect, growth ring pattern, and MOE_d measurements from the LVL material. Results suggested improved LVL F_t predictions could be achieved by integrating ultrasonic and optical systems. Additionally, the optical model, which included average defect, growth ring, and density measurements, better explained the variation in LVL static F_t values ($R^2 = 0.58$) compared with the MOE_d ($R^2 = 0.51$) and UPT ($R^2 = 0.31$) models.

Keywords: Optical scanning, laminated veneer lumber tensile strength, veneer, veneer defects, ultrasonic NDE, Douglas-fir veneer, nondestructive evaluation.

INTRODUCTION

Veneer for manufacturing wood-based composite products (eg laminated veneer lumber [LVL] and plywood) is generally evaluated and sorted based on specific criteria. Veneer used in manufacturing structural plywood for the US market has to meet a particular visual grade, which determines the final panel grade designation (NIST 2007). LVL, however, is less of a commodity product, compared with structural

* Corresponding author: david.devallance@mail.wvu.edu
† SWST member

plywood, and manufacturers have their own set of veneer grade designations. Regardless of the specific requirements, most manufacturers use some type of veneer grading system. Early grading was based on visual classification, later followed by automated stress wave grading, and in some instances, optical scanning systems. Typically, optical information (eg defect size) is used to assign a visual grade to veneer material. Very little research, however, has used veneer defect information to predict LVL strength properties.

Nondestructive evaluation (NDE) has been used for some time to assess wood product quality. Ross et al (1998) defined NDE as "the science of identifying the physical and mechanical properties of a piece of material without altering its end-use capabilities and using this information to make decisions regarding appropriate applications." The earliest use of NDE was grading and sorting wood products on a visual basis (Bodig 2000). By determining size, amount, and location of defects, lumber and veneer are categorized into different grades for both structural and nonstructural (appearance) use. More recent developments in NDE techniques involve using various methods to better predict wood stiffness and strength. Many NDE techniques exist, including electrical resistance, dielectric and vibrational properties, acoustical emission, wave propagation, and X-ray (Ross et al 1998).

In early LVL research, Kunesh (1978) described a lack of consistency in producing high grades of parallel-laminated veneer lumber for visually graded C and D veneer. In response to this, a Metriguard system (Model 239 Stress Wave Timer) was initiated to grade veneer. Stress wave scanning systems rely on the theory of how stress waves travel through materials and a generally accepted formula to calculate dynamic modulus of elasticity (MOE_d). With stress wave velocity (c) and estimated density, MOE_d is calculated as follows (Pellerin and Ross 2002; Lang et al 2003):

$$MOE_d = c^2 \times \rho \qquad (1)$$

where:

MOE_d = dynamic modulus of elasticity (Pa)

c = ultrasonic stress wave velocity (m/s)

ρ = density (kg/m^3)

Ultrasonic stress wave veneer grading systems decrease overall variability in strength and elasticity from billet to billet and production run to production run compared with visual human grading (Sharp 1985). Also, many researchers reported good correlation between ultrasonically graded veneer measurements of MOE_d and veneer and LVL elastic properties (Koch and Woodson 1968; Pellerin and Galligan 1973; McAlister 1976; Jung 1982; Hunt et al 1989; Logan 2000; Lang et al 2003). Past research, however, has not proven the ability of ultrasonic stress wave systems to increase LVL mean strength compared with traditional visual grading (Pieters 1979). Furthermore, past research results are conflicted about whether LVL strength properties can be predicted using ultrasonically determined properties. In particular, Kunesh (1978) reported that veneer longitudinal stiffness (measured with a dynamic stress wave system) and LVL tension and bending strength resulted in a correlation of 0.92 and 0.91, respectively. Jung (1982), however, reported that ultrasonic stress wave values correlated poorly with strength (R^2 from 0.004-0.306). Also, he reported that static MOE_s did not correlate well with static strength (R^2 from 0.081-0.371). Poor correlations between static MOE and static strength suggest that defects need to be considered when relating these two properties.

Jung (1979) reported stress wave techniques did not detect steep grain angles in veneer and knots in wide sheets. Gerhards (1982) indicated if straight grain was located around knots in lumber, overall knot influence on stress waves was minimal. Furthermore, Jung (1979) pointed out when measuring stress wave velocity only at veneer's end grain, defect location and size probably cannot be established. Based on Jung's

(1979) findings, current ultrasonic stress wave systems would not be able to estimate location and size of defects, which may be the limiting factor controlling veneer strength properties. Also, a gap exists in stress wave analysis systems because there is no theoretical relationship between MOE_s and various strength properties (Bodig 2000). Quantifying defects and growth ring patterns with optical scanning (ie machine vision) systems could improve prediction of LVL mechanical properties based on properties of veneer sheets comprising a billet.

With color camera systems, defects can be classified more efficiently than with grayscale optical systems (Brunner et al 1990; Boardman et al 1992; Lebow et al 1996). Boardman et al (1992) reported an optical system that combined signals of a three-color system (light–dark, red–green, and yellow–blue) and was able to detect defects in black walnut veneer at a 78% success rate. Brunner et al (1992) investigated Douglas-fir veneer and found only one-dimensional analysis (ie brightness) was required to detect knots but two-dimensional analysis (ie measures of brightness and chromaticity) was needed to identify multiple defects (eg knots and pitch streaks). Funck et al (1991) optically scanned Douglas-fir veneer sheets (0.61 m wide × 2.44 m long) and found ultrasonic propagation time (UPT) measurements could be predicted (R^2 of 0.77) using veneer defect area and latewood percentage obtained from optical imaging. Specifically, by applying a threshold to green channel signals, images were converted from color to black and white (ie binary), and then latewood and defect pixels were counted. Although these results were promising for development of an optical scanning system, their prediction model was only related to UPT and not mechanical properties of veneer. The relationship between defect measurements and LVL strength properties has not been studied in great detail. This research was designed to develop a nondestructive optical scanning system that includes defect and growth ring pattern measurements and predicts LVL tensile strength properties. Furthermore, the study investigated whether improvements in LVL tensile property prediction could be made by combining ultrasonically and optically determined measurements.

MATERIALS AND METHODS

Specimen Preparation

Forty-two ultrasonically graded 3.175-mm-thick, full-sized (≈1.27 m wide × 256.5 mm long) Douglas-fir (*Pseudotsuga menziesii*) veneer sheets were sampled from a local manufacturing facility. Sheets were selected based on MOE_d to represent typical grades used in manufacturing LVL (ie G1, G2, and G3). Fourteen sheets per grade were selected in such a way that each grade was adequately represented and high grading of the population did not occur. From each veneer sheet, 0.15-m-wide × 1.22-m-long specimens were prepared. A total of 310 specimens was randomly sampled and used to manufacture LVL, whereas other samples were used in a separate project. After being processed from full sheets, specimens were conditioned to equilibrium at 60% RH and 20°C.

Ultrasonic Testing

Small veneer specimens were tested for ultrasonic propagation time using a Metriguard (Pullman, WA) Model 239A laboratory-style stress wave timer, which was modified to include a pneumatically controlled clamping system (275.8 kPa) and a moveable table. The clamping system assured adequate and consistent contact pressure between the veneer surface and the stop and start accelerometers. The moveable table provided consistent linear movement at set points across the veneer. Prior to stress wave testing, specimen width (at three locations), thickness (at six locations), and weight were measured and recorded.

UPT (ie transit time) was then measured at six points across specimen width, the first reading taken 12.75 mm from the edge and in increments of 25.4 mm thereafter. At each location, only one measurement was taken. Based on earlier testing, UPT value did not significantly change (if at all) for this set when repeatedly tested at the same location. Start and stop gains on the stress wave timer were set at 4 and 40, respectively. Accelerometers were located 101.6 mm from specimen ends, thus resulting in an overall transit distance of 1.02 m. Individual UPT was measured and recorded. In addition, for each point at which UPT was determined, raw ultrasonic stress wave data were captured using a Tektronix (Beaverton, OR) 2430A digital oscilloscope and used for a separate portion of the study. For each specimen, UPT measurements were averaged. MOE_d was calculated for each specimen using Eq 1 and was based on velocity (ie final UPT divided by transit distance) and measured specimen density. No adjustment for moisture content was used because all veneer and LVL specimens used in the study were subjected to the same conditioning environment.

Optical Scanning

After ultrasonic testing, specimens were tested nondestructively using an optical scanning system. Each specimen was imaged using a Hitachi (Tokyo, Japan) HV-C20 video camera (with a Pentax 8-48 mm F/1.0 lens) connected to an AT&T Targa-32 image acquisition card. Both halogen (overhead lamps) and fluorescent (room) lighting were used to uniformly illuminate the veneer surface. Spatial resolution of approximately 5.11 and 4.66 pixels/cm along the length and across the width, respectively, was used when capturing images. After optical scanning, specimens were placed back in the conditioning chamber. Defects were identified from each image using ImageJ (Rasband 2009) through conversion of images to 8-bit grayscale followed by application of a maximum entropy threshold scheme. Only the portion of veneer (ie 0.61 m long × 0.15 m wide) that was going to be under tensile stress was analyzed. Resulting images were saved as bitmap files for determining defect and growth ring pattern measurements.

Defect area was determined using a program written in MATLAB® software (Mathworks 2009) that output the number of white (defect-free area) and black (defect area) pixels and calculated defect area percentage. Defect number and width were determined using Adobe Photoshop software (Adobe Systems Incorporated 2008). Defect volume (both for knots and holes and assuming a relatively circular shape) was then calculated based on average veneer thickness and defect width using the standard equation for cylinder volume. Captured images were also analyzed using proprietary software developed at Oregon State University, which output an edge-tracing grayscale image (ie entropy image) (Fig 1). An in-depth explanation of the algorithm and method used to output the entropy image can be found in Funck et al (2003). To measure growth ring patterns, entropy images were analyzed along the length and across the width (Direction 1 and 2, respectively, in Fig 1). Grayscale value of each individual pixel within a line along the entropy image's length and then across the width was summed and recorded. With the sum for each line within the entropy image, overall image statistics of mean, minimum, maximum, standarddeviation, and median were determined and recorded as measurements of growth ring pattern. Statistical values were determined for both Direction 1 (E) and Direction 2 (E90). The process of analyzing and calculating entropy image statistics was done using an automated process via a program written in

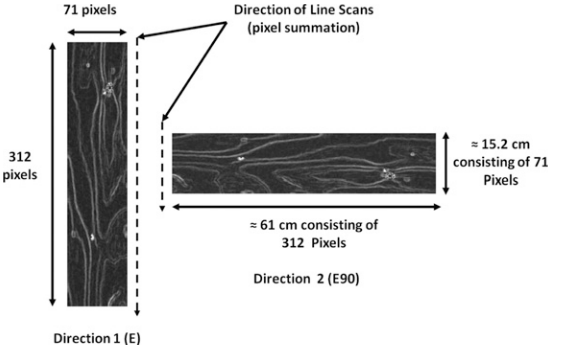

Figure 1. Growth ring pattern measurement images showing analysis along the veneer image length (E) and across the veneer width (E90).

MATLAB software. Further description of methods used to quantify defect and growth ring pattern measurements can be found in DeVallance (2009).

Laminated Veneer Lumber Assembly

Veneer specimens tested nondestructively were then randomly selected and manufactured into a specific layer in a particular LVL specimen. Each LVL specimen was comprised of five layers (nominal 15.875-mm total thickness). A total of 62 LVL specimens was manufactured. Each specimen was aligned parallel to achieve a loose-side to tight-side interface. Individual LVL specimens were stacked in a specially designed fixture and pressed to pressure (using a torque wrench) rather than final thickness, which simulated the pressing process of manufacturing facilities. Table 1 outlines process variables maintained throughout the LVL lay-up based on the adhesive manufacturer's recommendations for the emulsion polymer isocyanate adhesive used. After the 24-h cold pressing, each LVL specimen was processed into a tension specimen. Because some misalignment occurred during LVL manufacturing, specimens were edge-trimmed to a nominal width of 0.15 m and end-trimmed as long as possible to maximize grip area (≈1.2 m long). After 7 days of cold stacking, LVL tension specimens were conditioned to equilibrium at 60% RH and 20°C.

Laminated Veneer Lumber Specimen Nondestructive and Destructive Testing

After the LVL specimens reached equilibrium moisture content, they were first tested nondestructively. Ultrasonic testing was performed on final LVL specimens prior to tension testing. Procedures outlined previously for individual veneers were used to test LVL specimens. Transit time, again, was measured across 1.02 m. Ultrasonic testing was performed on LVL specimens at approximately the same locations as in individual veneer testing. After the nondestructive evaluation, LVL specimens were tested destructively in tension. Following procedures outlined in ASTM D4761 (ASTM 2005), axial tension static strength (F_t) was evaluated. Specimen width, thickness, and length were measured and recorded prior to testing each LVL specimen. Also, LVL specimen density (at the time of testing) was determined. LVL specimens were tested in tension parallel to grain at 6.35 mm per min of hydraulic ram motion. The grip area was set at ≈0.3 m on each end, leaving 0.61 m as the length between the variable thickness wedge-type grips. Testing was performed using a specially designed tension testing apparatus. Failure was generally achieved in 4 to 6 min. Load was measured by an Interface (Scottsdale, AZ) 890-kN load cell, and load at failure was recorded. After testing, static F_t was calculated. Also, specimen moisture content was evaluated following ASTM D4442; Method B (ASTM 2007).

Table 1. Outline of laminated veneer lumber specimen assembly process variables.

Manufacturing stage	Process setting
Raw material	Douglas-fir veneer at 11.5-12.5% MC (O.D. basis)
Adhesive application:	
Adhesive	WONDERBOND® EPI EL-70 with WONDERBOND® EPI CL-1
Adhesive viscosity	6000-6500 cP at 21°C
Application technique	Laboratory roller glue-spreader
Adhesive spread rate	293 g/m^2—single glue-line (60 lb, MSGL)
Stand time after adhesive application	Less than 20 min
Cold press	
Time	24 h
Temperature	Approximately 21°C
Pressure	1.21 MPa
Cold stacking	1 wk at approximately 21°C

RESULTS AND DISCUSSION

Laminated Veneer Lumber Test Results

Table 2 summarizes the destructively determined LVL static F_t. The coefficient of variation for LVL static F_t was slightly lower than the average 25% coefficient of variation reported for tensile parallel to grain of clear wood (FPL 1999). The coefficient of variation, however, was higher than the 10-12% for LVL when UPT was used as a sorting method (Sharp 1985). The higher coefficient of variation in this study was probably caused by purposely selected random veneer sorting rather than sorting to decrease the variation. This also suggests that some means of sorting (eg via average UPT) are likely to result in lower variation compared with random sorting.

Laminated Veneer Lumber Tensile Strength Prediction

LVL tensile strength (F_t) properties were analyzed to determine which NDE measurements were statistically significant in predicting tensile strength. Linear, variable selection (ie stepwise and all possible combinations), and multiple linear regression techniques were used to determine the most appropriate prediction equation models for static properties based on NDE measurements. It initially appeared that some variables were related in some prediction models. However, the variables were determined to be measuring different properties and were significant in predicting LVL F_t, thus there was no reason to exclude these variables (McDonald 2009). Further description of methods used in selecting the most appropriate optical scanning and combined system models can be found in DeVallance (2009). Prediction analysis was performed using average veneer measurements comprising an entire LVL specimen. In doing so, all ultrasonically and optically determined measurements for all five veneers within a specimen were averaged. Average ultrasonic, optical, density, and combined measurements were used to predict static LVL F_t.

Table 2. Laminated veneer lumber destructively determined tension test results.

Summary statistic	Density (kg/m^3)	MC (%)	F_t (MPa)
Average	541.4	12.0	40.1
Standard deviation	22.4	0.3	8.3
Coefficient of variation (%)	4.1	2.1	20.6
Minimum	490.2	11.4	21.0
Maximum	591.1	12.7	58.6
Sample size	62	62	62

The relationship between density and LVL mechanical properties was an important aspect for this research. Specifically, density was used in calculating MOE_d from ultrasonic testing and as a variable in portions of the optical system prediction models. Density has a relationship with various wood mechanical properties (FPL 1999). In this study, there was a relatively weak relationship between density and LVL F_t (R^2 = 0.372), indicating that density, by itself, was not very reliable in predicting LVL F_t. This suggests that other factors influence LVL F_t properties.

Results from ultrasonic system tests indicated average MOE_d (Model A) (R^2 = 0.509) was a better predictor of LVL static F_t values than UPT (R^2 = 0.309). Past research reported conflicting results for correlations between ultrasonically measured values and various LVL properties. When Model A was compared with LVL static F_t, results from this study showed a higher correlation than those reported by Jung (1982) (R^2 = 0.185) but a considerably lower correlation than results reported by Kunesh (1978) (R^2 = 0.92). Furthermore, actual NDE testing of LVL specimens, prior to tension testing, resulted in a relatively weak relationship between MOE_d and LVL static F_t (R^2 = 0.367). This research did demonstrate, however, that averaging individually measured veneer MOE_d values provided better prediction of LVL static F_t compared with actual nondestructive ultrasonic testing of LVL material. Although not specifically tested, this may show that ultrasonic stress waves are not greatly influenced by defects or other features located throughout various layers of LVL. It may be likely that stress waves travel only through surface layers when longitudinal stress wave testing is performed.

In terms of the optical scanning system, the prediction model including average optical and density measurements (Model B) performed slightly better than Model A. Regression results using average basic optical measurements and density (Model B), with no growth ring pattern measurements included, indicated five average characteristics were statistically significant (0.05 significance level) in predicting LVL static F_t (Table 3). In this regression, 52.5% of variation in LVL static F_t was explained by linear regression coefficients. Improvements were made to the optical system prediction model by incorporating growth ring pattern measurements. Specifically, regression results using the average of all optical measures (basic optical and growth ring pattern measurements) and density (Model C) indicated six average characteristics were statistically significant (0.05 significance level) in predicting LVL static F_t (Table 4). In this regression, 57.5% of variation in LVL F_t was explained by linear regression coefficients. In terms of the optical system, the model that included growth ring pattern measurements (Model C) performed better than Model A in explaining variation in LVL static F_t.

The model that best explained variation in LVL static F_t was obtained by combining measurements determined from optical and ultrasonic scanning systems (ie combined systems model) (Table 5). Specifically, regression results using combined system (ie average optical and MOE_d) measurements (Model D) indicated five average characteristics were statistically significant (0.05 significance level) in predicting LVL static F_t (Table 5). In this regression, 64.5% of variation in LVL static F_t was explained by linear regression coefficients. These results indicated LVL static F_t could best be predicted by combining average MOE_d and key optical values together. This finding suggests improved LVL F_t predictions could be achieved by integrating ultrasonic and optical systems already existing in many manufacturing facilities.

Table 6 summarizes how well each model explained variation in LVL static F_t. Statistical testing was used to evaluate which model was significantly better at predicting LVL static F_t. Specifically, a partial F-test was used to compare Model A and Model D because the two models were nested. The remaining

Table 3. Statistically significant variables, regression coefficients, and *p* values from regression analysis on average optical and density data for predicting laminated veneer lumber static tensile strength (MPa).

Independent variable	Regression coefficient	*p* value
Constant	−54.6	0.008
Average density (kg/m^3)	0.2243	0.000
Average number of defects	3.3950	0.028
Average total defect width (mm)	−1.3410	0.001
Overall average defect width (mm)	0.7296	0.027
Average total defect volume (mm^3)	0.0032	0.004

Table 4. Statistically significant variables, regression coefficients, and *p* values from regression analysis on average optical (including growth ring pattern measurements) and density data for predicting laminated veneer lumber static tensile strength (MPa).

Independent variable	Regression coefficient	*p* value
Constant	−50.5	0.015
Average density (kg/m^3)	0.1564	0.001
Average maximum defect width (mm)	1.9381	0.015
Average total defect width (mm)	−1.3452	0.000
Average total defect volume (mm^3)	0.0039	0.002
Average maximum defect volume (mm^3)	−1.0143	0.012
Average E minimum	0.0049	0.007

Table 5. Statistically significant variables, regression coefficients, and p values from regression analysis on combined system measures for predicting laminated veneer lumber static tensile strength (MPa).

Independent variable	Regression coefficient	p value
Constant	−10.9	0.293
Average dynamic modulus of elasticity (MPa)	0.0041	0.000
Average total defect width (mm)	−0.9527	0.001
Overall average defect width (mm)	0.5528	0.024
Average total defect volume (mm^3)	0.0027	0.006
Average E90 minimum	0.0124	0.021

Table 6. Comparison of R^2 values of developed models for predicting laminated veneer lumber static tensile strength.

Model type	Model	R^2
Predictions based on average veneer measurements in laminated veneer lumber specimens	Average ultrasonic propagation time	0.31
	Average density	0.37
	Average dynamic modulus of elasticity (Model A)	0.51
	Average basic optical + density (Model B)	0.53
	Average basic optical + density + GRP (Model C)	0.58
	Average combined systems (Model D)	0.65

GRP = growth ring pattern.

Table 7. Results of statistical comparisons among models for predicting laminated veneer lumber static tensile strength.

Model comparison[a]	Test	Test statistic[b]	p value	p value (reversed)[b]	Conclusion
Model D vs Model A	Partial F-test	5.485	0.0011	N/A	Model D fits significantly better than Model A
Model D vs Model B	J-test	N/A	0.0001	0.728	Model D fits significantly better than Model B
Model D vs Model C	J-test	N/A	0.0003	0.162	Model D fits significantly better than Model C
Model C vs Model B	J-test	N/A	0.0024	0.1175	Model C fits significantly better than Model B
Model C vs Model A	J-test	N/A	<0.0001	0.0013	Not statistically different
Model B vs Model A	J-test	N/A	0.0003	0.0011	Not statistically different

[a] Model A = average dynamic modulus of elasticity; Model B = average basic optical + density; Model C = average basic optical + density + growth ring pattern (GRP; and Model D = average combined systems.
[b] N/A = not applicable.

comparisons among models were evaluated using a J-test because the models were nonnested (Davidson and MacKinnon 1981). J-test statistical analysis was performed using SAS® software (SAS 2007). The J-test procedure tests whether one model is preferred when models are not nested within each other. The first step of the procedure is to fit both models in question. Then, the fitted value of the dependent variable from one model is used as an additional regressor in the other model and vice versa. Statistical significance of these parameters is used to assess whether one model fits significantly better than the other. For example, if the parameter on the fitted value of Model 1 is significantly different from zero in Model 2, but the parameter on the fitted value of Model 2 is not significantly different from zero in Model 1, then one can conclude that Model 1 outperforms Model 2.

Results for comparing each model's ability to predict LVL static F_t are shown in Table 7. Model D was significantly better at predicting LVL static F_t than the other three models. Regarding the optical system, the model that included growth ring pattern measurements (Model C) was significantly better at predicting LVL static F_t. Also, although optical system models (Models B and C) explained more variation, there was no statistically significant difference between the optical models and Model A in their ability to predict LVL static F_t. Developed optical systems, however, were as capable of predicting LVL static F_t as the ultrasonic system (ie Model A). Also, including growth ring measurements explained more variation when predicting LVL static F_t. From results of this study and analysis of specimen failure patterns, veneer defects and growth ring patterns were important factors that influenced LVL tensile strength. Given the results for predicting LVL static F_t when using average veneer measurements within a specimen, it was determined the optical system showed promise as a suitable method to predict LVL static F_t properties. Logan (2000) suggested optical systems could be effective in helping visual sorting but had not demonstrated a means of controlling veneer physical properties. The optical scanning system developed in this research appears to have bridged this gap of the inability of optical scanning to control veneer properties used in LVL. Specifically, this research proved the developed optical scanning system performed as well as the ultrasonic system when grading veneer and predicting LVL tensile mechanical properties. Further improvement in the optical system, in particular measurement of growth ring pattern angles and quantifying amount of diving grain, would probably improve the explanation of variability in LVL F_t values.

CONCLUSIONS

When combined with ultrasonic information, the developed optical system resulted in improved veneer grading and LVL mechanical property predictions. Specifically, Model D, which included overall average optical measurements, growth ring pattern measurements, and MOE_d of veneers comprising the LVL specimens, best explained variation in LVL static F_t values compared with all other models. Also, by using average measurements from the optical system, in conjunction with density, more of the variation in LVL static F_t was explained compared with Model A. Two optical system models (with density included) performed comparably with the MOE_d model. Furthermore, these two optical models explained more variation compared with nondestructive ultrasonic testing on actual LVL specimens when predicting LVL static F_t. Based on these findings, an optical system, which includes measurements of density, appears to show promise as an improved means of grading veneer for use in LVL compared with predictions based solely on MOE_d or UPT. To further improve the ability of the optical system to predict LVL tensile strength, research is needed to better quantify veneer growth ring patterns and diving grain.

It was evident that optically determined measurements improved the prediction of LVL tensile F_t. By including optical system measurements with density and ultrasonic information (ie combined system), improvements were made in veneer grading and LVL property predictions. With an optical system to locate and quantify veneer measurements, manufacturers of veneer composites (LVL and plywood) could improve final product properties. Specifically, by knowing the location and influence of specific veneer defects and characteristics, manufacturers would be able to make better decisions about veneer selection and placement within a composite. Also, optical scanning could benefit manufacturers after the final billet is produced. Current ultrasonic grading provides average property predictions of the entire LVL billet (which are typically 1.2 m wide by "x" long). LVL billets are then typically processed further into smaller width pieces. Resulting pieces are assumed to be equivalent to the average value of the LVL billet from which they were processed. Rather than using average properties from the billet, sorting processed LVL material based on optical measurements contained within the smaller piece could result in better predictions of LVL properties and improved sorting and grading. The optical system also could be used to sort products produced from downgraded LVL material, optimize defect randomization in LVL billets, and optimize ripping of material (eg flange stock) from billets. With information from an optical scanning system, manufacturers could better select and orient veneers to maximize product strength performance.

ACKNOWLEDGMENTS

Partial funding for this research was provided by a special grant from the USDA. Any opinions, findings, conclusions, or recommendations expressed are those of the authors and do not necessarily reflect the view of the U.S. Department of Agriculture. We acknowledge Dr. Ryan J. Luchs at Duquesne University for providing assistance with statistical analysis. Appreciation is also expressed to Freres Lumber Co., Inc., Hexion Specialty Chemicals, Murphy Engineered Wood Division, TECO, and Weyerhaeuser Company for providing assistance and materials. This manuscript is published with the approval of the Director of West Virginia Agricultural and Forestry Experimental Station as Scientific Article No. 3094.

REFERENCES

Adobe Systems Incorporated (2008) Adobe Photoshop software. Version 5.5. San Jose, CA.

ASTM (2005) D 4761-05. Standard test methods for mechanical properties of lumber and wood-base structural material. American Society for Testing and Materials, West Conshohocken, PA.

ASTM (2007) D 4442-07. Standard test methods for direct moisture content measurement of wood and wood-base material. American Society for Testing and Materials, West Conshohocken, PA.

Boardman BE, Senft JF, McCabe GP, Ladisch CM (1992) Colorimetric analysis in grading black walnut veneer. Wood Fiber Sci 24(1):99-107.

Bodig J (2000) The process of NDE research for wood and wood composites. Pages 7-22 *in* Proc 12th Int Symp Nondestructive Testing of Wood, September 13-15, 2000, Sopron, Hungary. University of Western Hungary, Sopron, Hungary.

Brunner CC, Maristany AG, Butler DA, VanLeeuwen D, Funck JW (1992) An evaluation of color spaces for detecting defects in Douglas-fir veneer. Industrial Metrology 2(3/4):169-184.

Brunner CC, Shaw GB, Butler DA, Funck JW (1990) Using color in machine vision systems for wood processing. Wood Fiber Sci 22(4):413-428.

Davidson R, MacKinnon JG (1981) Several tests for model specification in the presence of alternative hypotheses. Econometrica 49(3):781-793.

DeVallance DB (2009) Non-destructive evaluation of veneer using optical scanning and ultrasonic stress wave analysis systems. PhD Dissertation, Oregon State University, Corvallis, OR.

FPL (1999) Wood handbook: Wood as an engineering material. Gen Tech Rep FPL-GTR-113 USDA For Serv Forest Prod Lab, Madison, WI. 463 pp.

Funck JW, Brunner CC, Butler DA (1991) Softwood veneer defect detection using machine vision. Pages 113-120 *in* Proc Process Control/Production Management of Wood Products: Technology for the 90's Symposium. October 30 to November 1, 1990, Southeastern Section Annual Meeting, Athens, GA. Forest Products Research Society, Madison, WI.

Funck JW, Zhong Y, Butler DA, Brunner CC, Forrer JB (2003) Image segmentation algorithms applied to wood defect detection. Comput Electron Agric 41:157-179.

Gerhards CC (1982) Longitudinal stress waves for lumber stress grading: Factors affecting applications: State of the art. Forest Prod J 32(2):20-25.

Hunt MO, Triche MH, McCabe GP, Hoover WL (1989) Tensile properties of yellow-poplar veneer strands. Forest Prod J 39(9):31-33.

Jung J (1979) Stress-wave grading techniques on veneer sheets. Gen Tech Rep FPL-GTR-27 USDA For Serv Forest Prod Lab, Madison, WI. 10 pp.

Jung J (1982) Properties of parallel-laminated veneer from stress-wave-tested veneers. Forest Prod J 32(7):30-35.

Koch P, Woodson GE (1968) Laminating butt-jointed, long-run southern pine veneers into long beams of uniform high strengths. Forest Prod J 18(10):45-51.

Kunesh RH (1978) Using ultrasonic energy to grade veneer. Pages 275-278 *in* Proc 4th Symp on Nondestructive Testing of Wood, August 28-30, 1978, Vancouver, WA. Washington State University, Pullman, WA.

Lang EM, Bejo L, Divos F, Kovacs Z, Anderson RB (2003) Orthotropic strength and elasticity of hardwoods in relation to composite manufacture. Part III: Orthotropic elasticity of structural veneers. Wood Fiber Sci 35(2):308-320.

Lebow PK, Brunner CC, Maristany AG, Butler DA (1996) Classification of wood surface features by spectral reflectance. Wood Fiber Sci 28(1):74-90.

Logan JD (2000) Machine sorting of wood veneer for structural LVL applications. Pages 67-77 *in* Proc 34th Int Particleboard/Composite Materials Symp, April 4-6, 2000. Washington State University, Pullman, WA.

Mathworks (2009) MATLAB, Version 7.4. Natick, MA.

McAlister RH (1976) Modulus of elasticity distribution of loblolly pine veneer as related to location within the stem and specific gravity. Forest Prod J 26(10):37-40.

McDonald JH (2009) Handbook of biological statistics. 2nd ed. Sparky House Publishing, Baltimore, MD.

NIST (2007) Voluntary product standard PS 1-07, structural plywood. National Institute of Standards and Technology, Technology Administration, US Department of Commerce, Gaithersburg, MD. 52 pp.

Pellerin RF, Galligan WL (1973) Nondestructive method of grading wood materials. Canadian Patent No. 918286.

Pellerin RF, Ross RJ (2002) Nondestructive evaluation of wood. Forest Products Society, Madison, WI. 129 pp.

Pieters AR (1979) Ultrasonic energy: A new method for veneer grading. *in* Proc. ASCE Convention and Exposition. Preprint 3534, April 2-9, 1979, Boston, MA. 17 pp.

Rasband WS (2009) ImageJ. US National Institutes of Health, Bethesda, MD. http://rsb.info.nih.gov/ij/. 1997-2011. (Accessed 1/15/2011).

Ross RJ, Brashaw BK, Pellerin RF (1998) Nondestructive evaluation of wood. Forest Prod J 48(1):14-19.

SAS (2007) SAS Statistical Software, Release 9.2. Copyright 2002-2007. SAS Institute Inc., Cary, NC.

Sharp DJ (1985) Non-destructive testing techniques for manufacturing LVL and predicting performance. Pages 99-108 *in* Proc 5th Symp Nondestructive Testing of Wood, September 9-11, 1985. Washington State University, Pullman, WA.